EXHIBIT H

Process Safety and Environmental Protection 144 (2020) 186–192

Contents lists available at ScienceDirect

Process Safety and Environmental Protection

journal homepage: www.elsevier.com/locate/psep

Experimental study on thermal runaway and vented gases of lithium-ion cells

Liming Yuan*, Tom Dubaniewicz, Isaac Zlochower, Rick Thomas, Naseem Rayyan

Pittsburgh Mining Research Division, National Institute for Occupational Safety and Health (NIOSH), 626 Cochrans Mill Road, Pittsburgh, PA, 15236, United States

ARTICLE INFO

Article history:
Received 16 March 2020
Received in revised form 15 May 2020
Accepted 13 July 2020
Available online 17 July 2020

Keywords:
Lithium-ion battery
Temperature
Thermal runaway
Flammable gases

ABSTRACT

Lithium-ion (Li-ion) batteries have become more prevalent in mining to power a wide range of devices from handheld tools to mobile mining equipment. However, the benefits associated with using Li-ion batteries may come with a higher risk of a fire or an explosion. The major cause for a Li-ion battery fire is thermal runaway. If unmitigated, a thermal runaway can lead to cell rupture and the venting of toxic and highly flammables gases. Those flammable gases can cause a fire or explosion if ignited. In this study, researchers from the National Institute for Occupational Safety and Health (NIOSH) conducted experiments to monitor the heating of a Li-ion cell with different battery chemistries using an accelerating rate calorimeter (ARC). Inside the ARC, the cell was exposed to increasing temperatures until it reached a thermal runaway. Samples of vented gases after the thermal runaway were collected and analyzed using a gas chromatograph. Major gas components were identified, and their concentrations were measured. The results of this study can be useful in reducing the hazard of Li-ion battery fires.

Published by Elsevier B.V. on behalf of Institution of Chemical Engineers.

1. Introduction

The use of lithium-ion (Li-ion) batteries has become more widespread, from consumer electronic products to large power-consuming devices such as electric vehicles. As with other industries, the mining industry also sees the benefits of the efficient battery chemistries now available to power equipment in both coal mining and metal and non-metal mining operations. However, the benefits associated with using the Li-ion batteries may come with a higher risk of fire or explosions due to battery failure. The Occupational Safety and Health Administration (OSHA, 2019) reports that the U.S. Consumer Product Safety Commission identified over 25,000 overheating or fire incidents involving more than 400 types of lithium-battery-powered consumer products over a 5-year period. The safety issues pose a great challenge for the wider application of Li-ion batteries in large power-consuming devices. The major cause for catastrophic failure of Li-ion batteries is thermal runaway that occurs when heat generated from exothermic reactions inside a battery outpaces heat dissipated from the battery leading to a rapid increase in temperature and pressure that further increases the reaction rate. If unmitigated, this self-accelerating process will lead to cell rupture and the venting of toxic and highly flammable gases, and the release of heat. An ignition of those flammable gases can lead to a possible explosion or fire. An explosion scenario can be more severe for a large battery, where the heat generated by one failed cell can heat up neighboring cells and lead to a thermal cascade throughout the battery.

Li-ion battery thermal runaway can be caused by exposure to excessive temperatures, internal shorts due to cell defects, external shorts due to faulty wiring, a surge in the charging or discharging current, or mechanical damage to the cell that can lead to internal shorts and heat generation. Much research has been conducted to examine the fire and explosion hazards of Li-ion batteries caused by thermal runaway (Chen et al., 2015, 2019; Chen et al., 2020; Kong et al., 2018; Somandepalli et al., 2014) and to study the contributions of the different cell chemistries and materials, and failure initiation mechanisms to thermal runaway (Chen et al., 2016; Liu et al., 2016; Quintiere, 2020; Wang et al., 2017). Wang et al. (2012) reviewed the Li-ion battery hazards, thermal runaway theory, basic reactions, thermal models, and the related prevention techniques. Although the general thermal runaway theory is available, the physical and chemical processes occurring during thermal runaway are complex. Different electrode materials, electrolytes, and cell types exhibit different thermal runaway behaviors. The reactions at different thermal runaway stages are dependent upon the

* Corresponding author at: Fires and Explosions Branch, Pittsburgh Mining Research Division, National Institute for Occupational Safety and Health (NIOSH), 626 Cochrans Mill Road, Pittsburgh, PA, 15236, United States.
E-mail address: Lcy6@cdc.gov (L. Yuan).

https://doi.org/10.1016/j.psep.2020.07.028
0957-5820/Published by Elsevier B.V. on behalf of Institution of Chemical Engineers.

component materials (cathode, anode, separator, electrode binder, and electrolyte), state of charge, and discharge rate. Ponchaut et al. (2015) quantified the vent gas composition, heat generation, and overpressure resulting from the combustion of vent gases released during a thermal runaway of a soft-pack pouch cell. Fernandesa et al. (2018) identified and quantified gases emitted during abuse tests by overcharge of a commercial Li-ion battery. Wu et al. (2018) conducted a thermal stability evaluation of materials in a soft-pack commercial cell including anode, cathode, and separator for a fully charged cell under both internal heating and external heating modes. Larsson et al. (2018) studied gas explosions and thermal runaways during external heating or physical abuse of commercial Li-ion cells at different levels of ageing. Ribiere et al. (2012) investigated the fire-induced hazards of Li-ion cells. Larsson et al. (2017) researched toxic fluoride gas emissions from Li-ion battery fires.

These studies focused on the quantification of toxic and flammable gases and heat generated during the thermal runaway, and identification of the fire and explosion hazard of the vented gases for a single cell that is often used for consumer electronic products. The emphasis was on the wide variety of cell types involving a lithium metal oxide cathode and a lithium/graphite anode. These studies provided a necessary database for understanding of the safety hazard of such Li-ion batteries. However, for battery-powered mining equipment, different battery chemistries may be used. The Global Mining Guidelines (GMG) Group (2017) identified battery chemistries representative of those being used for mining vehicles—cells with an iron phosphate cathode (LFP), cells with a nickel manganese cobalt cathode (NMC), and cells with a titanate anode (LTO). This paper presents the experimental results of cell heating to thermal runaway and analyses of the vented gases of Li-ion cells with LFP, NMC, and LTO battery chemistries. Major gas components of vented gases are identified and related concentrations are determined using a gas chromatograph. The results of this study can be useful in reducing the hazard of Li-ion battery fires for battery-powered equipment.

2. Experimental methods

Li-ion battery thermal runaway experiments were conducted using an accelerating rate calorimeter (ARC) made by Thermal Hazard Technology (THT). Accelerating rate calorimetry is a powerful technique used to study the thermal behavior of Li-ion cells under different conditions (Gnanaraja et al., 2003). ARC measurements are useful for obtaining onset temperature points of self-heating and the temperature, pressure, and cell destruction consequences of thermal runaway reactions of Li-ion batteries. In this study, the ARC system comprising an EV + and a standard ARC was used to conduct thermal runaway tests. Each Li-ion cell was sealed within a canister placed within the ARC. The canister consisted of a capped 5-cm (2-inch) diameter (nominal) schedule 80 steel pipe with an internal volume of 220 cm^3. Another canister with an internal volume of 735 cm^3 was used for multiple cell tests. The ARC gradually heated the canister and cell using a ramp heating mode with a heating power of 4.9 kW until the cell reached thermal runaway. A thermocouple was attached to the cell surface to measure its temperature, while the pressure and temperature inside the canister were monitored using a pressure transducer and a thermocouple. Before each test, the cell was conditioned with three charge-discharge cycles followed by charging to the 100 % state. The charge and discharge rate of the battery was C/4, and the ambient temperature was roughly 25 °C. The THT ARC enhanced system (ARCes) control and data acquisition software recorded sensor data every 0.6 s. The collected gas samples after a thermal runaway were analyzed using a gas chromatograph (GC) from Agilent (7890 Series) to quantify the major components of the dried vented gas. To examine the thermal stability of battery cell components, fully charged cells of different chemistries were disassembled, and small samples of the cell anodes, cathodes, and separators were removed from the cell body and analyzed using a differential scanning calorimetry (DSC) from TA Instruments. The component was run without the presence of electrolyte. The DSC tests were conducted at a heating rate of 10 °C per minute using dry, purified air as the sweep gas.

Table 1
Summary of cell characteristics.

Cell type	Size	Cell weight, g	Rated capacity, Ah	Nominal voltage, v
LFP	26,650	90.1	3.8	3.2
LTO	18,650	38.6	1.3	2.4
NMC 1	18,650	45.3	3.2	3.67
NMC 2	18,650	45.2	3.2	3.67

Three types of commercial Li-ion cells were selected for testing in the ARC. One type has a lithium nickel manganese cobalt (NMC) cathode and a graphite anode with cells from different manufacturers, designated as NMC 1 and NMC 2; one type of cell has a lithium iron phosphate (LFP) cathode and a graphite anode, designated as LFP; and one type has a lithium titanate (LTO) anode, designated as LTO. Table 1 summarizes the cell weight, rated capacity, and nominal voltage for those cells. Each battery test was repeated twice to ensure test repeatability, and a total of 18 ARC tests were conducted.

3. Results and discussion

3.1. Cell component thermal analysis

Thermal analysis results using the DSC on the cell anodes are shown in Fig. 1. For both NMC cells, there was a sharp exothermic peak. For NMC 2, the exothermic peak occurred at 159 °C, while it occurred at 174 °C for NMC 1 cell. For the LTO cell, there was only a small endothermic peak and heat flow, while there was a weak, broad endothermic peak for the LFP cell. Fig. 2 shows DSC analysis results for different cell cathodes. Both NMC cell cathodes experienced exothermic reactions over a wide range of temperatures—from 125 to 200 °C. The peak value occurred at 156 °C for NMC 2 and 166 °C for NMC 1. The LFP and LTO cathodes experienced the endothermic reactions only with two peaks. The first peak occurred around 145 °C, while the second one occurred around 189 °C. The DSC results for different separators are shown in Fig. 3. NMC 1 and NMC 2 had much higher peak heat flow values, indicating that more heat was released during the oxidation. The NMC 1 separator had an exothermic peak heat flow value at 152 °C. The exotherm had a relatively broad and flat peak. Both NMC 1 and NMC 2 separators had an endothermic peak heat flow value at 138 °C indicating a possible shutdown feature of the separators. The DSC results indicate that NMC 1 and NMC 2 anodes, and cathodes were less thermally stable than those for LFP and LTO.

3.2. Cell heating

During the ARC tests, battery cell surface temperatures increased as the cell was exposed to the continuous heating from the heaters located on the top, side, and bottom of the calorimeter. Fig. 4 shows the typical cell temperature and pressure in the ARC test for an LFP cell using the 220 cm^3 canister. The cell surface temperature increased slowly at a rate of about 1.6 °C/min. The pressure inside the canister increased slowly as well. When the cell surface temperature reached 182 °C, the temperature suddenly dropped about 2 °C because of the vent opening of the battery. This vent opening led to the release of some gases into the canister causing a significant pressure rise from 1.9 to 4.5 bar. After the vent

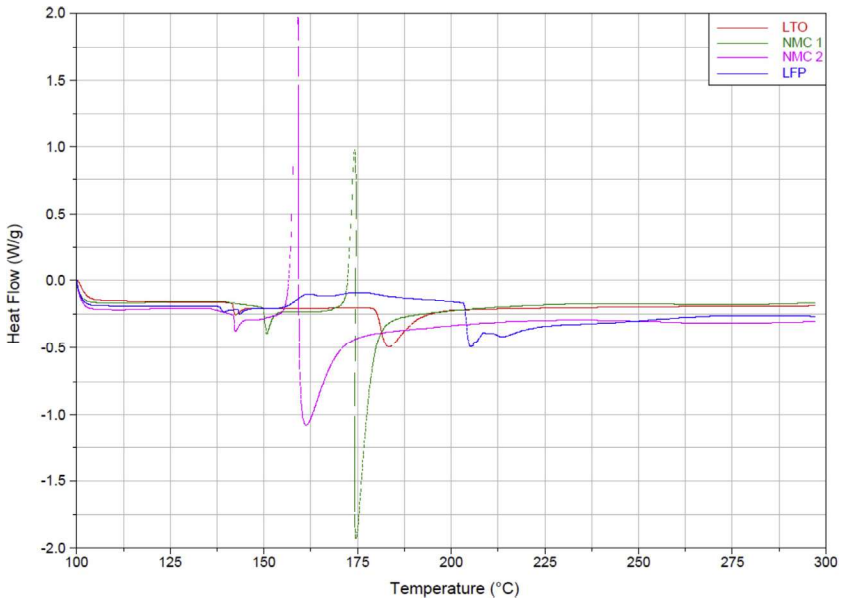

Fig. 1. DSC analysis of different anodes.

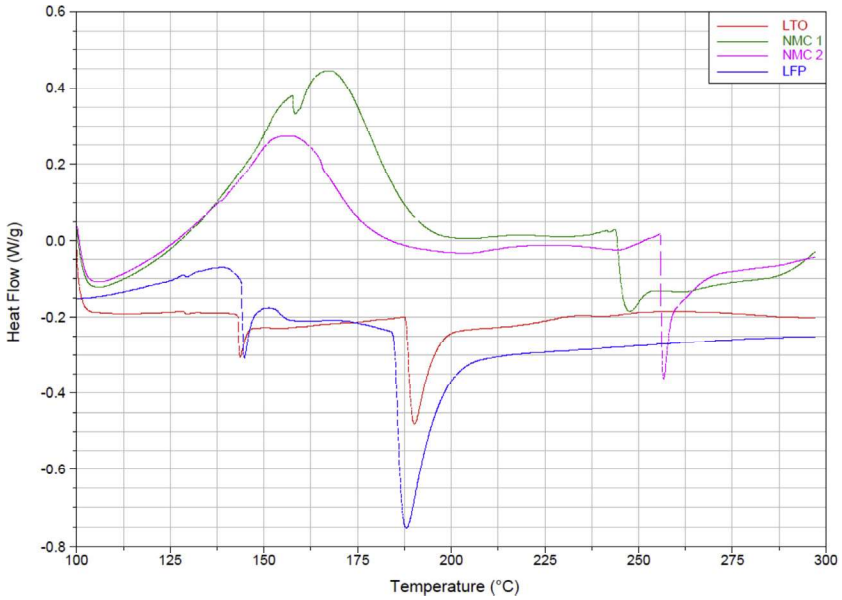

Fig. 2. DSC analysis of different cathodes.

opening, the cell surface temperature continued to increase slowly. When the temperature reached above 200 °C, a thermal runaway occurred leading to a very fast temperature and pressure rise. The peak surface temperature reached 399 °C with a maximum temperature rise rate over 85.5 °C/s. The peak pressure reached 31.6 bar with a peak pressure rise rate of 290 bar/s.

Fig. 5 compares the surface temperatures during ARC tests for the four cells featuring different electrode compositions and/or suppliers. The ARC heating of battery cells was terminated when the temperature inside the ARC reached 180 °C. When the cell temperature reaches a certain characteristic value, thermal runaway occurs, i.e. the onset temperature of the auto-accelerating thermal runaway reactions. The NMC 2 cell exhibited a relatively slow rise to the onset temperature for thermal runaway (exceeded only by the LFP cell which also had a somewhat higher onset temperature), but produced the highest peak temperature of 998 °C. The LTO cell exhibited a faster temperature increase rate to thermal runaway but produced the lowest peak temperature of 305 °C. The NMC 1 cell reached the thermal runaway condition the fastest, and its peak runaway temperature (over 800 °C) was exceeded only by NMC 2.

The comparison of canister pressures for different cells is shown in Fig. 6. The NMC 2 cell produced the largest pressure, 101.6 bar, while the LTO cell had the lowest pressure of 28.8 bar. It is worth noting that the two NMC cells produced about three times the peak pressure of the LFP and LTO cells. It should be pointed out that the LFP cell has a larger cell size of 26650 (26 mm in diameter and 65 mm in length) leading to a smaller free space inside the canister. An 18650 (18 mm in diameter and 65 mm in length) LFP cell produced a peak pressure of 16.8 bars in the same test. The peak pressures from NMC 2 and NMC 1 cells dropped very quickly, which may reflect a rapid extinguishment of the flame from the thermal runaway. Such a flame emission was observed in cell tests conducted without a canister in the ARC, so that the cell thermal runaway could be videotaped during the test. It was observed that a flame was

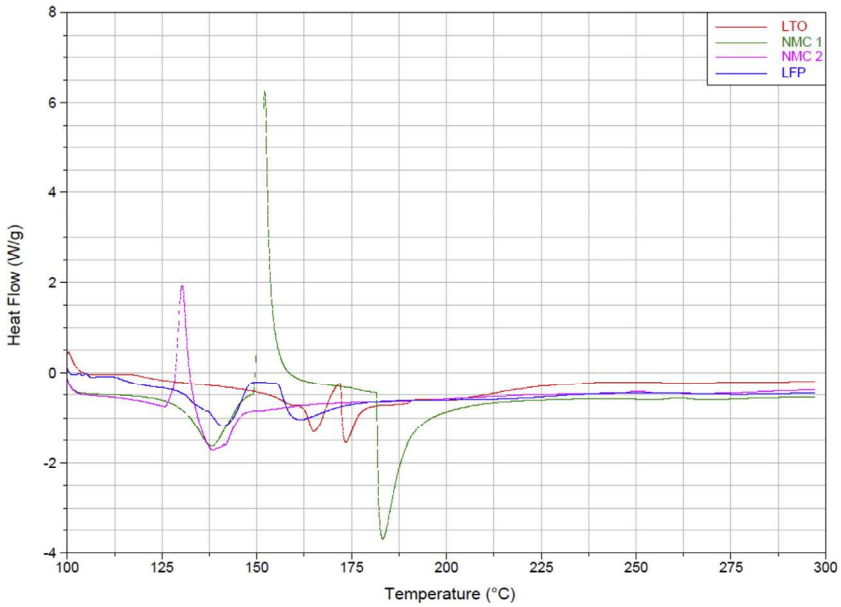

Fig. 3. DSC analysis of different separators.

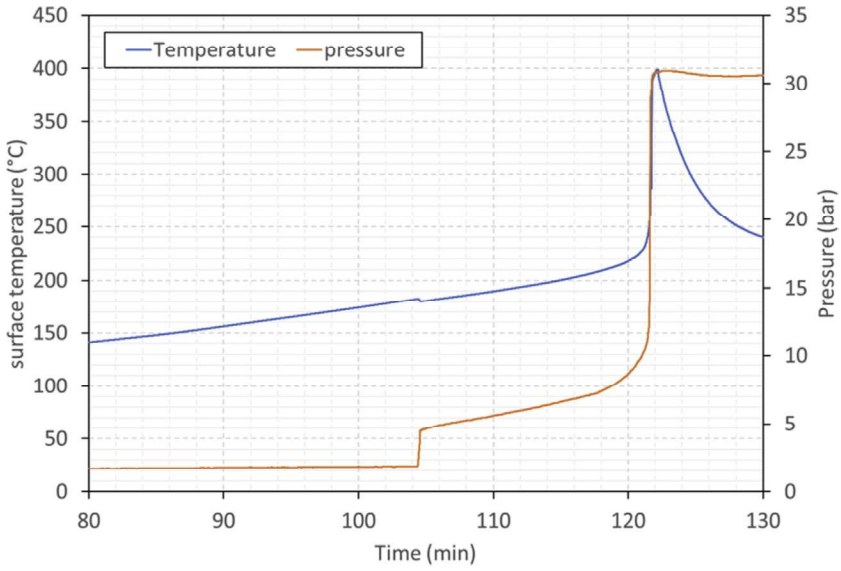

Fig. 4. Typical cell temperature and pressure in the ARC test for an LFP cell.

Table 2
Summary of onset temperatures and peak temperatures.

Battery chemistry	Onset temperature (°C)	Peak cell temperature (°C)	Peak gas temperature (°C)
LFP	200	399	275
LTO	163	305	245
NMC 1	145	835	244
NMC 2	140	998	313

emitted by the NMC 18650 cell during its thermal runaway, while only smoke was emitted from the LFP cell during a corresponding test. For LFP and LTO cells, the pressure decreased slowly after the thermal runaway as the canister cooled and because of suspected condensation of some product water and residual cell solvent.

Table 2 summarizes the onset temperatures and peak cell temperatures for different cells. The results for the NMC and LFP cells are consistent with those reported in the literature (Golubkov et al., 2014). Although the LTO cell exhibited a lower onset temperature than the LFP cell, it also had a lower peak cell temperature. The NMC cells had the lowest onset temperatures and highest peak temperatures, indicating higher thermal instability than the cells with the more stable cathode (LFP) or anode (LTO). These results are consistent with the findings of Lei et al. (2017) on the experimental analysis of thermal runaway in 18650 Li-ion cells with different cathode materials. Their tests confirmed that cells with an LFP cathode exhibited good stability under thermal abuse, while cells with an NMC cathode featured greater safety issues at high temperatures.

3.3. Amounts of vented gases

The amount of gas inside the canister during the ARC test can be calculated by applying the ideal gas law:

Case 1:21-cv-00704-JLS-HKS Document 78-1 Filed 06/09/25 Page 6 of 8

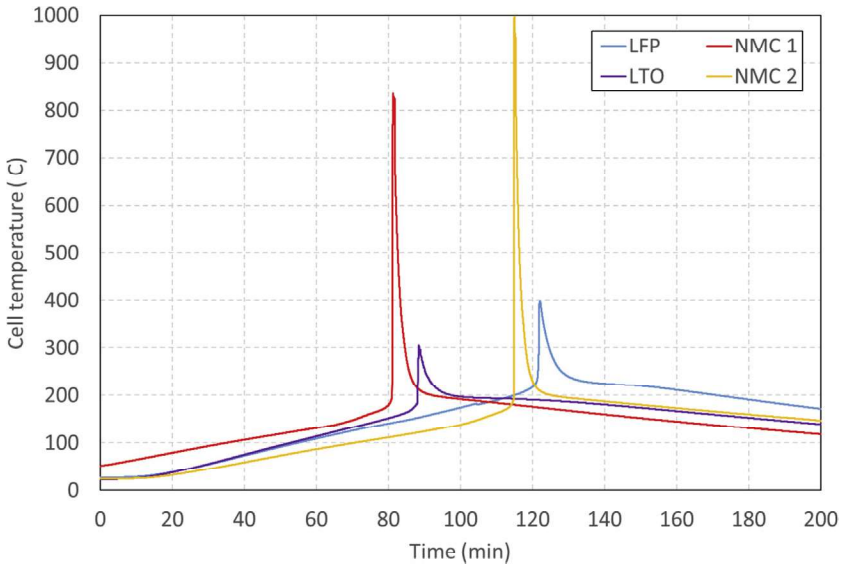

Fig. 5. Comparison of surface temperatures during ARC tests for four cells.

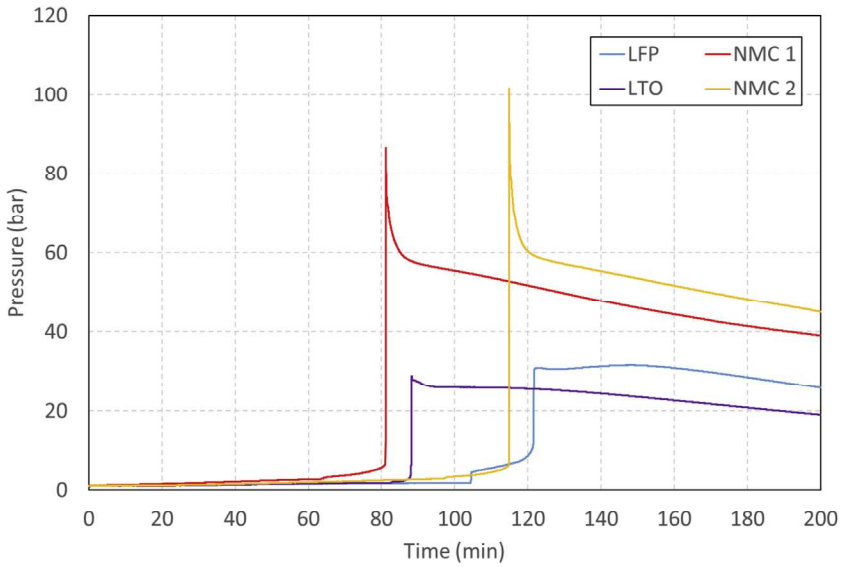

Fig. 6. Comparison of pressures during ARC tests for four cells.

$$n = PV/RT$$

Where n is number of moles of all gases inside the canister, P is the pressure inside the canister in bar, V is the free space of the canister, 203.5 cm^3 for the 18650 cell and 185.5 cm^3 for the 26650 cell, R is the gas constant, 83.145 cm^3 bar/mol·K, and T is the gas temperature in K. The gas temperature inside the canister was much lower than the cell surface temperature during the thermal runaway. The peak gas temperatures are shown in Table 2. The NMC 2 cell had the highest peak gas temperature of 313 °C, while the NMC 1 and LTO cells had the lowest peak gas temperatures of 244 °C. The moles of vented gas equal the number of gas moles during the ARC test minus the original gas moles in the canister. The moles of vented gases for different cells are compared in Fig. 7. Both NMC cells released much higher amounts of gas than the LFP and LTO cells. In fact, the trend of gas moles followed that of the pressure profiles. Table 3 lists the volumes of vented gas at ambient temperature and pressure and the normalized gas volumes for the different cells. The LTO cell had the lowest amount of vented gas volume of 3.20 L, while the NMC 2 cell had the highest amount of 11.08 L. However, the LFP cell had the lowest weight-normalized gas volume, 36.5 L/kg. The LFP value is close to the value reported by Sturk et al. (2019) for the same type cell.

Table 3
Summary of vented gas volumes and normalized gas volumes.

Battery chemistry	Vented gas volume	Normalized gas volume
LFP	3.29 L	36.5 L/kg
LTO	3.20 L	82.9 L/kg
NMC 1	9.77 L	215.17 L/kg
NMC 2	11.08 L	245.1 L/kg

The amounts of vented gas in Table 3 is for a single cell reaching a thermal runaway. In practice, multiple cells may undergo thermal runaway during a battery fire incident. To quantify the amount of vented gas for multiple cells as a function of their number, ARC tests were conducted with more than one cell placed in a larger canister that has a volume of 735 cm^3. This canister can host one to three

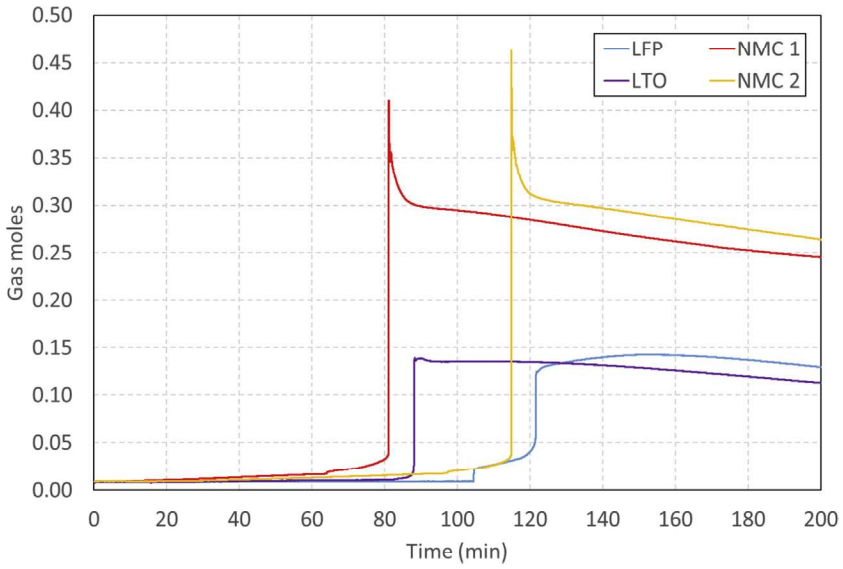

Fig. 7. Moles of vented gases for different cells.

Table 4
Vented gas volumes of multiple LFP cells.

Number of cells	Peak pressure, bar	Vented gas volume	Peak cell temperature, °C
1	11	3.79 L	263
2	25	8.98 L	360
3	34	11.72 L	432

separated LFP 26650 cells. Three battery thermal runaway tests were conducted with one, two, and three LFP 26650 cells placed in the canister, respectively. The peak pressures, vented gas moles, and peak cell temperatures are summarized in Table 4. As the larger canister was used in these tests compared to those tests shown in Figs. 5 and 6, the pressure and temperature values cannot be compared with those using a smaller canister for the same LFP cell. The gas volumes (converted to ambient temperature and pressure) for the single LFP cell using both canisters are very close. The experimental data on vented gas volumes for two and three cells indicate that the vented gas volume was approximately proportional to the number of cells when the cells were under the same confinement and heating abuse conditions.

3.4. Components of vented gases

Table 5 summarizes the concentrations of major gases from gas chromatograph (GC) analyses for vented gases with different battery chemistries. The samples were diluted with Helium 5:95. Each diluted sample was run three times. The results were averaged, corrected for dilution, and the percent deviation calculated. The percent deviation for these gases is from 15.78 to 29.72 %. Except for CO_2, all other gases are flammable, while CO is also toxic. These GC tests performed could not detect trace gases that may be toxic even in low quantities. The gas composition was significantly dependent on the battery chemistry as two NMC cells produced similar gas components. The LFP cell produced the highest levels of H_2, C_2H_2, C_2H_4, and C_2H_6, but lowest for CO. The NMC cell produced the highest levels of CO and CH_4, but the lowest levels of C_2H_4 and C_2H_6. The LTO cell produced the highest levels of CO_2 and lowest levels of H_2, CH_4, and C_2H_2. The release of sufficient quantities of flammable gases (e.g. H_2, CH_4, C_2H_2, C_2H_4, C_2H_6, and CO) can create a fire or explosion hazard when the flammable gases mix with atmospheric oxygen and form a flammable fuel-air mixture.

In a mine environment such as in underground metal and nonmetal mines, a ventilation airflow with velocity of 1~2 m/s is usually available for the dilution of flammable and toxic gases from a Li-ion battery thermal runaway. However, if the battery is used on surface or in a space, it is important to provide an appropriate airflow to dilute those flammable gases to below the lower explosive limits, 4% for H_2 and 5% for CH_4. The CO concentration needs to be diluted below 50 ppm to prevent any gas poisoning.

4. Conclusions

Four types of Li-ion battery cells with three different chemistries that are promising for mining industry application were tested using the ARC to study the cell heating rates under external heat and gases vented during the thermal runaway. The experimental results demonstrate that the NMC cells had the lowest onset temperature for a thermal runaway and produced the highest cell temperature and largest amount of vented gases leading to the highest pressure. The LTO cell had the lowest maximum cell temperature and produced the least amount of vented gas leading to the lowest maximum gas pressure. The LFP cell had a slightly higher onset temperature, producing the maximum gas temperature, and gas pressure. The DSC analyses of cell components (anodes, cathodes, and separators) indicate that NMC cells were less thermally stable than those for LFP and LTO. However, the major gas concentrations of vented gases were mainly dependent on the battery chemistry.

Table 5
Summary of GC analyses of vented gases.

Battery chemistry	H_2 (%)	CO (%)	CO_2 (%)	CH_4 (%)	C_2H_2 (%)	C_2H_4 (%)	C_2H_6 (%)
LFP	24.34	4.5	25.39	5.9	0.08	3.26	1.29
LTO	8.41	5.3	37.6	1.23	0.0008	1.38	0.40
NMC 1	12.39	30.30	13.22	10.50	0.0026	0.10	0.16
NMC 2	12.54	28.06	19.91	12.90	0.0027	0.16	0.21

Under conditions in this study, the H_2 concentration inside the canister ranged from 8.41 to 24.34 %, CO concentration ranged from 4.5–30.3%, and CH_4 concentration ranged from 1.23 to 12.90 % indicating a potential safety and health hazard for mine workers should such a battery fire/explosion incident occur.

Disclaimer

The findings and conclusions in this report are those of the authors and do not necessarily represent the official position of the National Institute for Occupational Safety and Health, Centers for Disease Control and Prevention. Mention of any company or product does not constitute endorsement by NIOSH.

Declaration of Competing Interest

The authors declare that they have no known competing financial interests or personal relationships that could have appeared to influence the work reported in this paper.

Acknowledgements

The authors wish to thank David Stoker of Mine Safety and Health Administration (MSHA) Pittsburgh Safety and Health Technology Center for performing the GC analyses of four gas samples and also thank John Soles and Wei Tang for their help with the experiments.

Appendix A. Supplementary data

Supplementary material related to this article can be found, in the online version, at doi:https://doi.org/10.1016/j.psep.2020.07.028.

References

Chen, M., Zhou, D., Chen, X., Zhang, W., Liu, J., Yuen, R., Wang, J., 2015. Investigation on the thermal hazards of 18650 lithium ion batteries by fire calorimeter. J. Therm. Anal. Calorim. 122, 755–763.

Chen, M., He, Y., Zhou, D., Wang, J., He, Y., Yuen, R., 2016. Experimental study on the combustion characteristics of primary Lithium batteries fire. Fire Technol. 52, 365–385.

Chen, M., Ouyang, D., Weng, J., Liu, J., Wang, J., 2019. Environmental pressure effects on thermal runaway and fire behaviors of lithium-ion battery with different cathodes and state of charge. Process. Saf. Environ. Prot. 130, 250–256.

Chen, S., Wang, Z., Wang, J., Tong, X., Yan, W., 2020. Lower explosion limit of the vented gases from Li-ion batteries thermal runaway in high temperature condition. J. Loss Prev. Process Ind. 63, 103992.

Fernandesa, Y., Brya, A., dePersisb, S., 2018. Identification and quantification of gases emitted during abuse tests by overcharge of a commercial Li-ion battery. J. Power Sources 389, 106–119.

GMG, 2017. Recommended Practices for Battery Electric Vehicles in Underground Mining. Global Mining Guidelines (GMG), Ormstown, QC, CA, 20160726_UG_Mining_BEV-GMSG-WG-v01-r01.

Gnanaraja, J.S., Zinigrada, E., Asrafa, L., Gottlieba, H.E., Sprechera, M., Aurbacha, D., Schmidtb, M., 2003. The use of accelerating rate calorimetry (ARC) for the study of the thermal reactions of Li-ion battery electrolyte solutions. J. Power Sources 119–121, 794–798.

Golubkov, A.W., Fuchs, D., Wagner, J., Wiltsche, H., Stangl, C., Fauler, G., Voitic, G., Thaler, A., Hacker, V., 2014. Thermal-runaway experiments on consumer Li-ion batteries with metal-oxide and olivine-type cathodes. RSC Adv. 4, 3633–3642.

Kong, L., Li, C., Jiang, J., Pecht, M.G., 2018. Li-ion battery fire hazards and safety strategies. Energies 11, 2191.

Larsson, F., Andersson, P., Blomqvist, P., Mellander, B.E., 2017. Toxic fluoride gas emissions from lithium-ion battery fires. Sci. Rep. 7, 10018.

Larsson, F., Bertilsson, S., Furlani, M., Albinsson, I., Mellander, B.E., 2018. Gas explosions and thermal runaways during external heating abuse of commercial lithium ion graphite-$LiCoO_2$ cells at different levels of ageing. J. Power Sources 373, 220–231.

Lei, B., Zhao, W., Ziebert, C., Uhlmann, N., Rohde, M., Seifert, H.J., 2017. Experimental analysis of thermal runaway in 18650 cylindrical Li-ion cells using an accelerating rate calorimeter. Batteries 3, 14.

Liu, X., Wu, Z., Stoliarov, S., Denlinger, M., Masias, A., Snyder, K., 2016. Heat release during thermally induced failure of a lithium ion battery: impact of cathode composition. Fire Saf. J. 85, 10–22.

OSHA, 2019. Preventing fire and/or explosion injury from small and wearable lithium Battery powered devices. In: Safety and Health Information Bulletin SHIB 06-20-2019. Occupational Safety and Health Administration (OSHA).

Ponchaut, N., Marr, K., Colella, F., Somandepalli, V., Horn, Q., 2015. Thermal runaway and safety of large lithium-ion battery systems. In: Battcon International Stationary Battery Conference, Orlando, FL, May 12-14.

Quintiere, J.G., 2020. On methods to measure the energetics of a lithium ion battery in thermal runaway. Fire Saf. J. 111, 102911.

Ribiere, P., Grugeon, S., Morcrette, M., Boyanov, S., Laruelle, S., Marlair, G., 2012. Investigation on the fire-induced hazards of lithium-ion battery cells by fire calorimetry. Energy Environ. Sci. 5, 5271–5279.

Somandepalli, V., Marr, K., Horn, Q., 2014. Quantification of combustion hazards of thermal runaway failures in Lithium-Ion Batteries. SAE Int. J. Alt. Power 3, 98–104.

Sturk, D., Rosell, L., Blomqvist, P., Tidblad, A.A., 2019. Analysis of Li-ion battery gases vented in an inert atmosphere thermal test chamber. Batteries 5, 61.

Wang, Q., Ping, P., Zhao, X., Chu, G., Sun, J., Chen, C., 2012. Thermal runaway caused fire and explosion of lithium ion battery. J. Power Sources 208, 210–224.

Wang, Q., Huang, P., Ping, P., Du, Y., Li, K., Sun, J., 2017. Combustion behavior of lithium iron phosphate battery induced by external heat radiation. J. Loss Prev. Process Ind. 49, 961–969.

Wu, T., Chen, H., Wang, Q., Sun, J., 2018. Comparison analysis on the thermal runaway of lithium-ion battery under two heating modes. J. Hazard. Mater. 344, 733–741.